# Influence of the operational conditions on static and dynamic stiffness of rail pads

*Jose A. Sainz-Aja[(1)*], Isidro A. Carrascal[(1)], Diego Ferreño[(1)], Joao Pombo[(2,3)], Jose A. Casado[(1)], Soraya Diego[(1)].*

*(1) LADICIM (Laboratory of Science and Engineering of Materials), University of Cantabria. E.T.S. de Ingenieros de Caminos, Canales y Puertos, Av. Los Castros 44, Santander, 39005, Spain.*

*(2) Institute of Railway Research, University of Huddersfield, UK*

*(3) IDMEC, Instituto Superior Técnico, Universidade de Lisboa, Portugal and ISEL, IPL, Portugal.*

*Corresponding author.

## Highlights

- Full-scale characterization of fastening systems under in-service conditions.
- Temperature increments notably reduce rail pad stiffness.
- Toe load increments significantly increase rail pad stiffness.
- Axle load increments increase rail pad stiffness.
- Frequency increments slightly increase rail pad stiffness

## Abstract

*The track has a crucial role in the performance of the rail network as it provides support and guidance to the rolling stock. During train operation, the vehicle-track interaction generates high impact loads and fatigue, which lead to degradation of vehicle components and rail infrastructure. These loads tend to increase the maintenance needs and, consequently, the life-cycle-costs of the rail assets. In order to minimize these consequences, rail pads are generally used between the rails and the sleepers in order to provide flexibility to the track and to damp the transmission of noise and vibrations. In ballasted tracks, this flexibility is a combination of the mechanical properties of the ballast and the rail pads. However, in slab tracks, the flexibility of the infrastructure is almost exclusively dependent on the rail pads. These materials exhibit non-linear, dissipative characteristics that are affected by the service conditions such as temperature, frequency, toe load and axle load. This work aims to investigate experimentally different pad materials widely used in the rail industry in order to characterize the influence of these factors on the mechanical characteristics of the rail supporting elements. The detailed characterization of the rail pads enables not only better understanding of their performance in realistic service conditions, but also provides good perspectives for use of these well quantified mechanical properties in studying the vehicle-track dynamic behaviour in different scenarios and predicting the long-term performance of the infrastructure components.*

***Keywords:*** *Rail pad, dynamic stiffness, temperature, axel load, toe load, frequency.*

## 1. Introduction

The health and long-term performance of the infrastructure are critical in any rail system, not only due to safety aspects, but also owing to the high maintenance costs involved. Moreover, it is extremely important to minimize any disturbance in the railway service given the social and economic repercussions. Despite its importance, the performance and maintenance

management of the track are, scientifically, among the least understood and least predictable elements of railway systems. To try to tackle this situation, the analysis of the track structure and of its dynamic response has attracted the attention of many researchers aiming to support the rail industry in its developments (Indraratna et al., 2013).

The vertical track stiffness is widely regarded as the variable with most influence on the quality of the railway service, maintenance and durability (Chen and Zhou, 2020; Peltokangas and Nurmikolu, 2015; Xin et al., 2020). In conventional ballasted tracks (Sañudo et al., 2017), this parameter depends on the stiffness of the rail pads and, to a lesser degree, on the stiffness of the ballast layer. However, the ongoing tendency towards slab track systems (Chen and Zhou, 2020; Esveld, 2003; Sainz-Aja et al., 2019), especially for high-speed operations, means the rail pad is solely responsible for providing adequate vertical stiffness to the track . Xin et al. stated that without appropriate track transition, abrupt changes in track stiffness can cause accelerated degradation of track quality, requiring frequent maintenance and providing poor comfort (Xin et al., 2020). Actually, the variation of dynamic stiffness as experienced by the moving axles, is decisive in comfort and durability (Li et al., 2019, 2017; Sadri et al., 2019)".

Sol-Sánchez et al. (Sol-Sánchez et al., 2015) concluded that the use of softer rail pads produced larger rail deflection, which could lead to fatigue in this component or others such as the fastener system, although the low stiffness of rail pads protected the elements below. Moreover, a soft rail pad will have higher impact attenuation capacity, so damage will be reduced not only to the elements below the rail pad but also to switch points (Markine et al., 2011). Chen and Zhou concluded that improvement in the fastener stiffness can reduce the displacement of the rail, while increasing the displacement of the track and subgrade substructure. Therefore, it is crucial to control the fastener stiffness to ensure safe operation of high-speed trains."(Chen and Zhou, 2020). The use of more flexible rail pads reduces the transmission of noise and vibrations to the lower layers of the infrastructure and, consequently, their damage. In addition, these elements smooth the stiffness variations that occur in transitions such as bridges and tunnel entrances and exits. The use of stiffer rail pads has several advantages such as lower rail deflection and less energy consumption. It also reduces the rail displacements and accelerations, increasing the lifespan of the fasteners and attenuating the noise and vibrations created by the rails (Ferreño et al., 2019). Kaewunruen et al. (Kaewunruen and Remennikov, 2006) also pointed out that the stiffness of the pad influenced the resonance frequency of the sleepers, which can lead to their premature failure.

The rail pads are manufactured with materials that exhibit large non-linear and dissipative mechanical characteristics (Sadeghi et al., 2020), which are highly influenced by the loading and environmental conditions. The specialized literature confirms that pad stiffness depends on the excitation frequency (Cukrowicz et al., 2013; Fenander, 1997), on the mean load (Kaewunruen and Remennikov, 2007), on the loading amplitude (Wei et al., 2016; Zhu et al., 2015) and on the temperature (Wei et al., 2017b). In particular, Kai et al. (Wei et al., 2016) observed that vertical stiffness in TPE rail pads increased with load amplitude. Similarly, Zhu et al. (Zhu et al., 2015) reported that both hysteresis and stiffness augmented after increasing the frequency. Fenander (Fenander, 1997) studied the pads' response observing that the stiffness increases significantly with preload and, more moderately, with frequency. Wei et al. (Wei et al., 2017b) analysed the impact of frequency and temperature on the vertical stiffness of the soft under baseplate pad of WJ-8 rail fasteners concluding that the increase in frequency and the reduction in temperature led to an increase in stiffness.

Given the great importance of rail pads, an appropriate mechanical characterization is essential. The relevant literature exhibits a very specific profile, focused on very particular materials and/or working conditions. The main contribution of this work is the use of meticulous and exhaustive experimental campaigns to characterize the most widely used rail pads, considering the influence of all relevant variables involved. In particular, three pads manufactured in EPDM (Ethylene Propylene Diene Monomer), TPE (Thermopolymer Polyester Elastomer - HytrelTM) and EVA (Ethylene-Vinyl Acetate) were tested. Five static and 240 dynamic tests were performed to characterize each of these three materials, combining five different temperatures (-35, -20, 0, 20 and 52 °C), four different frequencies (2.5, 5, 10 and 20 Hz), four toe loads (1, 9, 18 and 25 kN) and three axle loads (6.2, 8.4 and 12.4 ton), corresponding to load amplitudes of 15.5, 21 and 31.5 kN.

Accurate characterization of the rail infrastructure components, where the rail pads have a significant role due to their relevance in the overall performance of the track, has great importance in vehicle-track interaction studies. Rail pad accurate characterization open up the possibility of integrating more detailed wheel-rail contact models (Marques et al., 2019; Pombo et al., 2007; Pombo and Ambrósio, 2008) and of considering track irregularities (Pombo and Ambrósio, 2012; Vollebregt and Steenbergen, 2015) and other track singularities (Coleman et al., 2012; Fortunato et al., 2013) in the studies with the aim of assessing track performance and degradation evolution (Iwnicki and Bevan, 2012; Stichel et al., 2014) in realistic operation conditions. More specifically, it is foreseen that the rail pad properties characterized here could be integrated into calibrated slab track models proposed in (Sainz-Aja et al., 2020) to build realistic track models in several operation scenarios. These reliable models can then be used together with detailed vehicle models, in a co-simulation environment, to study the long-term behaviour of the rail infrastructure and train components. Such an approach enables the development of suitable track and vehicle degradation models, which can be used to provide information for decision support tools, promoting the implementation of science-based maintenance strategies. This methodology overcomes the limitations of the conventional approach used by the rail industry that identifies degradation and deterioration by performing periodic inspections, which are disruptive and not very effective.

# 2. Rail Pads

The rail fastening is the system used to fix the rails to the sleepers, as shown in Figure 1. It not only prevents the rails from rotating, but also provides elasticity to the track and damps the transmission of noise and vibrations to the infrastructure when trains pass. In general, the rails are supported by sleepers through one or more plates called rail pads. These can be composed of different materials, namely, plastic, rubber or metal.

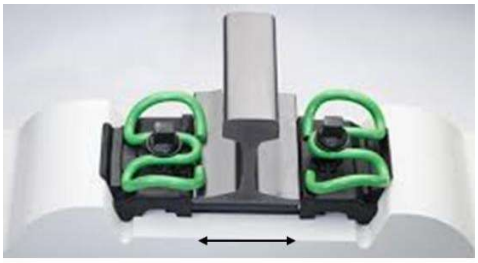


*Figure 1: Example of how the fastening system fixes the rail to the sleeper*

Under in-service conditions, the loading amplitude and frequency of the rail pads depends on the speed and axle-load of the train running on the track. The mean compressive force on the pads is a combination of the toe load and the weight of the trains. A reference value for the toe load is around 18 kN. Nevertheless, this value can vary due to excessive or insufficient torque during fastening/tightening or as a result of a sheath creep phenomenon. In an extreme scenario, the breakage of the fastening will result in the inexistence of the toe load.

The European standards EN 13481-2 and EN 13146-9 standards require the rail pads to be mechanically characterised at a temperature of 23 ± 5 °C. In addition, the mean value and amplitude of the loads are also fixed. It is therefore evident that the real in-service conditions of the pads can differ greatly from these ideal experimental conditions defined in the standards. This has consequences in the mechanical characteristics of the rail pads, e.g. their stiffness, which is strongly affected by temperature. Consider, for example, temperature differences between the high-speed line Medina-Mecca though the Saudi Arabian desert and Hanover–Würzburg line in Germany. In addition, it should be noted that, as a consequence of climate change, both average and, particularly, extreme temperatures of rail service are gradually increasing.

It is clear that not only the vertical stiffness of the rail pads is of vital importance for the track performance, maintenance and durability, but it is also essential to have an accurate description of the mechanical behaviour of these components in order to predict the vehicle-track interaction forces. In this work, three of the most commonly used rail pads are analysed. They are shown in Figure 2 and their main characteristics are summarized as follows:

- EPDM: It is a synthetic rubber plate without protrusions, with 7 mm thickness and a hardness of 21 HS-D. This solution is adopted, e.g., by the Saudi Arabian high-speed railways. This is the rail pad used in the W14 HHR fastening system.
- TPE: It is a medium stiffness thermoplastic with oblong shaped protrusions, 7 mm thickness and a hardness of 47 HS-D. It is used, for example, on PAE-2 rail pads (ADIF, 2005a), which are currently used in the Spanish high-speed railways. This is the rail pad used in the VM-SKL-1 fastening system.
- EVA: It is a stiff plastic pad without protrusions, with 6 mm thickness and a hardness of 46 HS-D. This solution was adopted in the first Spanish high-speed line between Madrid and Sevilla. This is the rail pad used in the HM-SKL-1 fastening system.

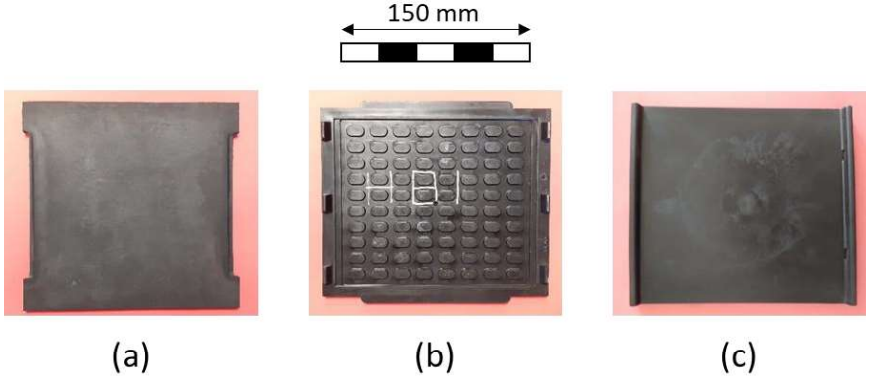


*Figure 2: Rail pads analysed: (a) EPDM rail pad; (b) TPE rail pad; (c) EVA rail pad*

# 3. Experimental Campaign

This work was aimed at experimentally determining the influence of temperature, load amplitude, frequency and toe load on the vertical stiffness of three of the most commonly used rail pads, EPDM, TPE and EVA. To this end, static and dynamic stiffness tests were performed to characterize the rail pads following the European standards EN 13146-9 and EN 13481-2. This combination of parameters resulted in a total of 15 static and 720 dynamic stiffness tests (240 dynamic tests for each pad). A summary of the parameters analysed in this study is shown in Table 1. Figure 3 describes the loading parameters: toe load, amplitude and frequency. Toe load is the compressive load applied by the fastening system which is used to hold the rail in position, its standard value is 18 kN but overtightening or undertightening is not a rare event in practice. In the limit case, the fracture of the fastening clip will release the toe load. It corresponds to the minimum force ($F_{min}$) during the loading cycle. The load amplitude simulates the passage of the train. The axle load of the train, is four times this load amplitude (two wheels and two times the load amplitude), the load amplitudes defined in the standard: 15.5, 21.0 and 31.5 kN results in 6.2, 8.4 and 12.6 Tm/axle respectively. Finally, the frequency modifies the period of the wave and is associated with the train speed. Consider that the velocity of a conventional train is ~200 km/h and of a current high-speed train is ~350 km/h. With a distance between bogies of 18 m, this corresponds to a frequency between 3 and 5 Hz. In order to assess the influence of high frequencies, an experimental range between 2.5 and 20 Hz was selected.

Figure 3: Load parameters definition

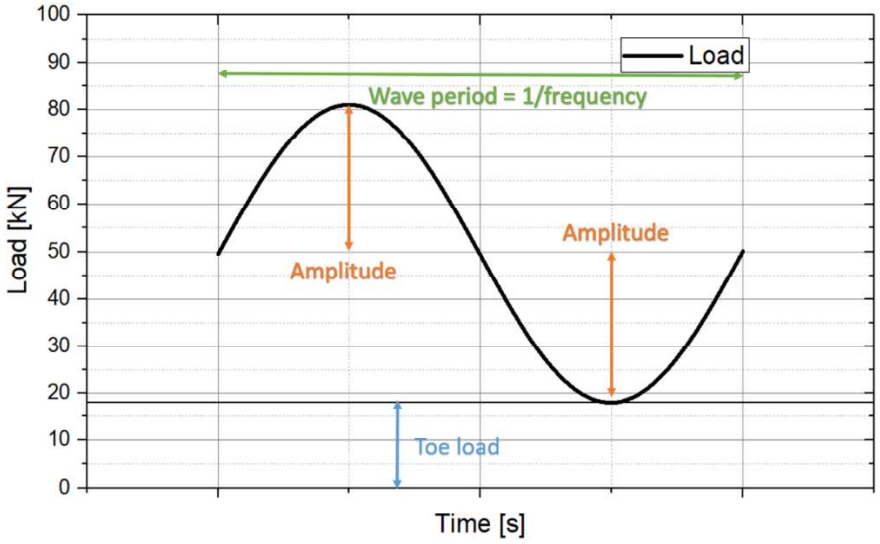


*Figure 3: Load parameters definition*

*Table 1: Parameters analysed in the experimental studies*

| Temperature [°C] | Axle Load Amplitude [kN] | Toe load [kN] | Frequency [Hz] |
|---|---|---|---|
| -35 | 15.5 | 1 | 2.5 |
| -20 | 21.0 | 9 | 5 |
| 0 | 31.5 | 18 | 10 |
| 20 | | 25 | 20 |
| 52 | | | |

The tests were carried out using different temperatures, starting from room temperature 23 ± 5 °C defined in standards. Then tests were conducted at the maximum (52°C) and minimum (-35°C), temperatures defined in the Spanish instructions on action to be taken in road bridge projects EHE-08. Additionally, in order to use similar temperature intervals, two additional intermediate temperatures, -20 °C and 0 °C, were also included. This range of temperatures enables to analyse high speed rail present in winter cold countries such as Denmark, Sweden, Norway and Finland, as well as in the Saudi Arabian desert (high-speed line between Medina and Mecca).

Stiffness tests were performed with a universal servo-hydraulic testing machine equipped with a load cell with a capacity of ± 100 kN. The deformation of the rail pads was measured by 4 LVDTs (Linear Variable Differential Transformers) located on a metallic base that simulates the geometry of the sleeper, as shown in Figure 4. The loads were applied to the rail pads by means of a UIC60 rail sample, which was connected to the test machine by means of a ball joint to ensure the verticality of the applied load, see Figure 4 (c) (ADIF, 2005b). During the stiffness tests, the vertical load and rail pad deformation were recorded, the latter as the average of the four LVDTs. Once the setup was placed inside the environmental chamber, the target temperature was maintained for one hour to ensure that the entire volume of the rail pad reaches the target temperature. The test apparatus for the extreme temperatures of -35 and 50 °C is shown in Figure 4.

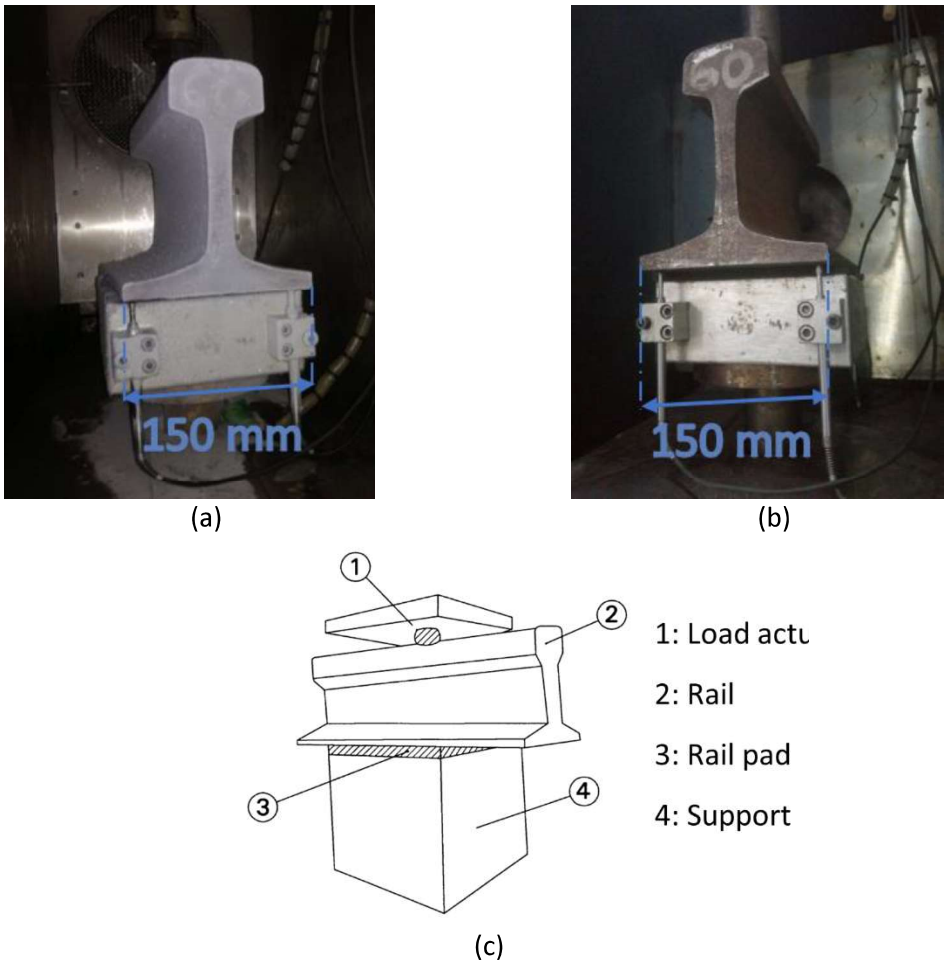


*Figure 4: Experimental setup of the stiffness tests conducted at: (a) -35°C; (b) 52°C (c) scheme of the test device*

As defined in standards EN 13481-2 and EN 13146-9, the pads static stiffness was determined by applying three loading and unloading ramps between 1 and 90 kN, with a speed of 2 kN/s, as shown in Figure 5(a). The dynamic stiffness was obtained by applying 1000 sinusoidal load cycles to the rail pad as depicted in Figure 5(b). The force-displacement curves that have to be recorded to determine the static and dynamic pad stiffnesses are shown in Figure 6(a) and (b), respectively.

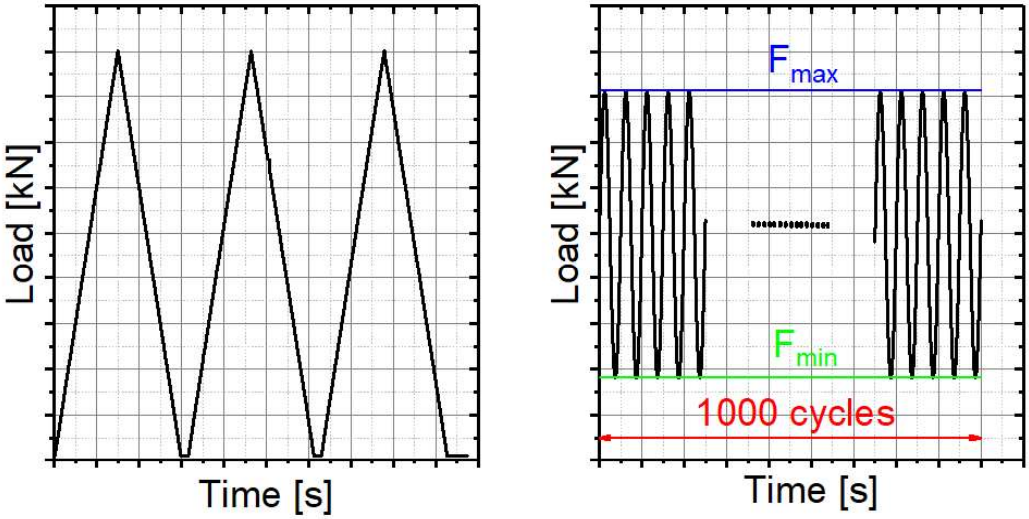


(a) (b)

*Figure 5: Procedures used to determine the static (a) and dynamic (b) pad stiffnesses*

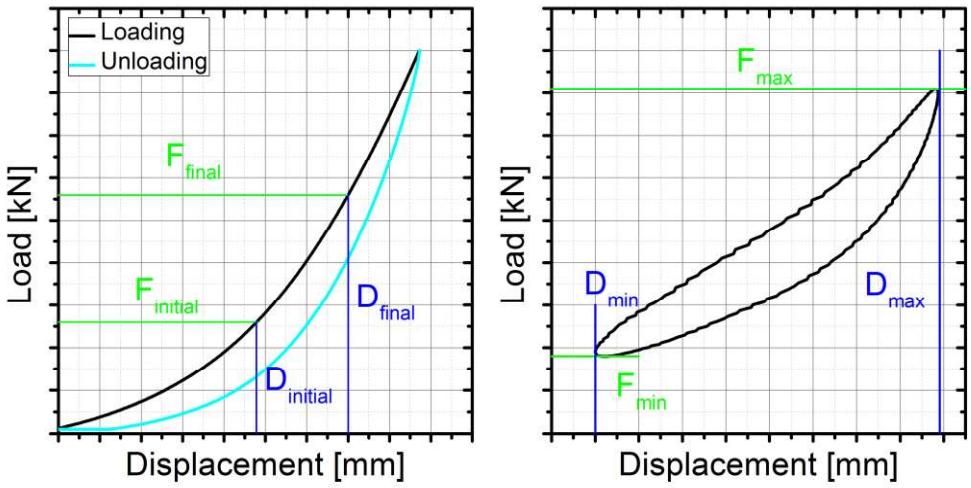


(a) (b)

*Figure 6: Force-displacement curves necessary to obtain the static (a) and dynamic (b) pad stiffnesses*

The static stiffness, $k_{st}$, was obtained as the ratio between the load range and the displacement range during the last load ramp, as shown in Figure 6(1)(a), and written as:

$$k_{st} = \frac{F_{final} - F_{initial}}{D_{final} - D_{initial}} \quad (1)$$

A new definition of static stiffness is proposed in this study, called relative stiffness $(k_{st})_r$. It is obtained by substituting the initial force and displacement of the static stiffness by the values corresponding to the toe load $F_{TL}$ and $D_{TL}$, written as:

$$(k_{st})_r = \frac{F_{max} - F_{TL}}{D_{max} - D_{TL}} \quad (2)$$

The dynamic tests were performed to determine the influence of several service conditions on pad stiffness, in addition to the temperature mentioned above for static stiffness tests. Specifically, the influence of the toe load, loading frequency and load amplitude were analysed. The dynamic stiffness of the rail pads was obtained as the ratio between the average load range and the average displacement range of the last 100 cycles of each test, written as:

$$k_{dyn} = \frac{\overline{F_{max}} - \overline{F_{min}}}{\overline{D_{max}} - \overline{D_{min}}} \quad (3)$$

The dynamic tests were carried out using the three amplitudes defined in standard EN 13481-2, which depend on the track category: 15.5, 21.0 and 31.5 kN, respectively. Four frequencies were also analysed, three of them defined in EN-13146-9: 5 (5.0, 10.0 and 20.0 Hz). Additionally, tests were performed at 2.5 Hz as in previous studies (Sainz-Aja et al., 2020). Finally, regarding the toe load, four scenarios were considered. First, the situation corresponding to a correct assembly of the system, i.e., 18 kN. Then, an extreme case of 1 kN, which represents the breakage of the fastening system. Finally, two additional conditions were considered derived from possible under-torque or over-torque of the fastening, corresponding to 9 and 25 kN, respectively. From these parameters, plus the temperature, the experimental campaign necessary for each rail pad's characterisation could be defined.

To analyse the influence of each of the four parameters (temperature, axle load amplitude, load frequency and toe load) on the vertical stiffness of the rail pads, the influence coefficient, CI, is defined as:

$$CI = \frac{Ri}{R_{HS}} \quad (4)$$

where $R_{HS}$ is the stiffness obtained under reference conditions for high-speed railway, i.e., with a toe load of 18 kN, axle load amplitude of 31.5 kN, frequency of 5 Hz and temperature of 20 °C as defined in the standards EN 13146-9 and EN 13481-2. $R_i$ is the stiffness obtained after changing only one of the parameters, maintaining the others in reference conditions. In this way, an influence coefficient CI≈1 means that the corresponding parameter has a negligible influence when compared with the reference conditions. On the contrary, CI>>1 and CI<<1 mean that the parameter has stiffening and flexibilization effects, respectively, on the pads.

# 4. Results and Discussion

## 4.1. Static Characterization

The force-displacement curves of the three pads under reference conditions are shown in Figure 7. The differences in the mechanical behaviour of the rail pads are evident. The EPDM rail pad undergoes a much greater deformation than the other two rail pads, especially in the initial region of the curve, below 50 kN. Beyond this force value, EPDM exhibits a significant stiffening.

EVA is the least deformable rail pad and its deformation is concentrated in the initial region, up to 20 kN. The behaviour of TPE is between EPDM and EVA and barely displays any stiffening. These findings are in line with the results previously obtained by other authors (Carrascal et al., 2018).

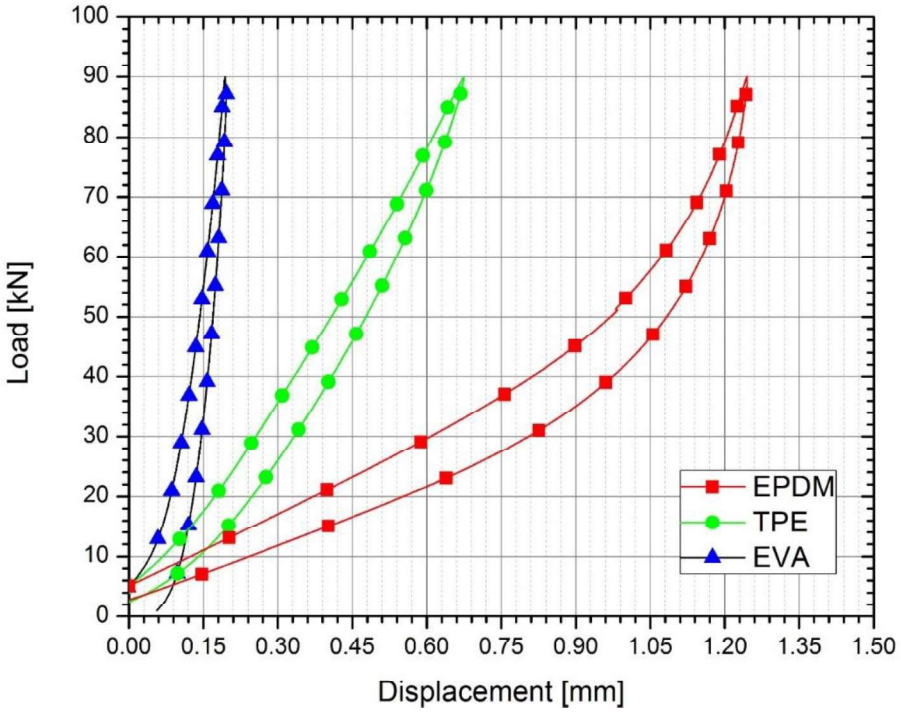


*Figure 7: Force-displacement curves of the static stiffness tests for the three rail pads under reference conditions*

Figure 8 shows, for each rail pad, the influence of temperature on the force-displacement curves, considering the reference conditions for toe load and load amplitude.

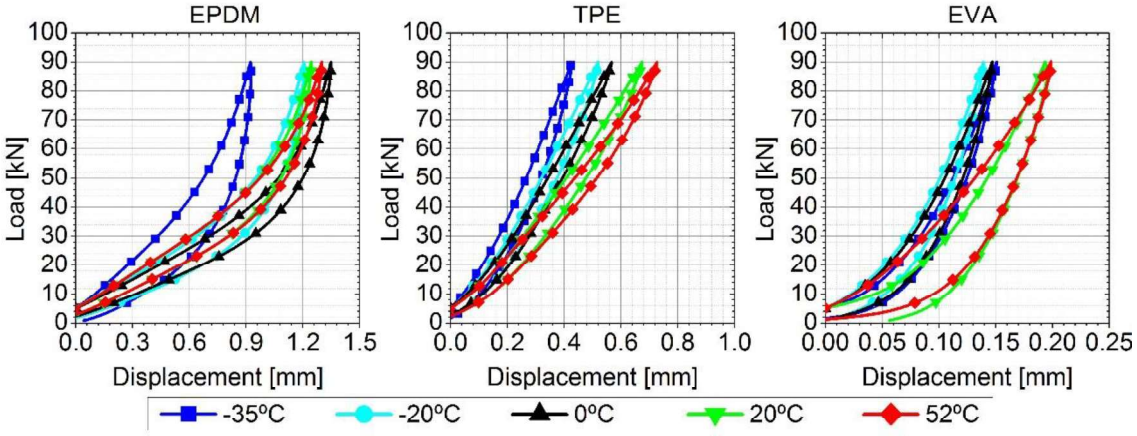


*Figure 8: Influence of temperature on static stiffness for reference conditions*

In general, as the temperature increases, the stiffness of the rail pads decreases. At a microscopic level, molecular mobility is enhanced by temperature, facilitating the deformation of the rail pads. In the case of EPDM, it can be seen that, for temperatures higher than -20°C, the shift of the curves is small and gradual. Nevertheless, a large increase in the stiffness occurs between -20°C and -35°C. The increase in stiffness undergone by TPE when reducing the temperature is gradual over the whole range between 52°C and -35°C. In the case of the EVA

pad, a noticeable increase in flexibility occurs between 0°C and 20°C with two clearly differentiated groups of curves above and below this gap.

Figure 9 shows the relative stiffness, defined in equation (1), as a function of the load for the three rail pads. Each of the curves corresponds to one tested temperature considering a toe load of 18 kN ($F_{initial}$) and an increasing load range ($F_{final}=F_{final}+F_{range}$). As can be seen, the greater the loading, the higher is the relative stiffness. Even though the stiffness of the three rail pads reduces as temperature rises, they display particular behaviours after being exposed to temperature variations. In EPDM the stiffness increases substantially at -35 °C and the differences between the curves in the range between -20 °C and 50 °C are negligible. In contrast, TPE progressively stiffens as temperature decreases. In EVA the stiffness is approximately constant between -35°C and 0°C but decreases substantially at 20 °C and 50 °C.

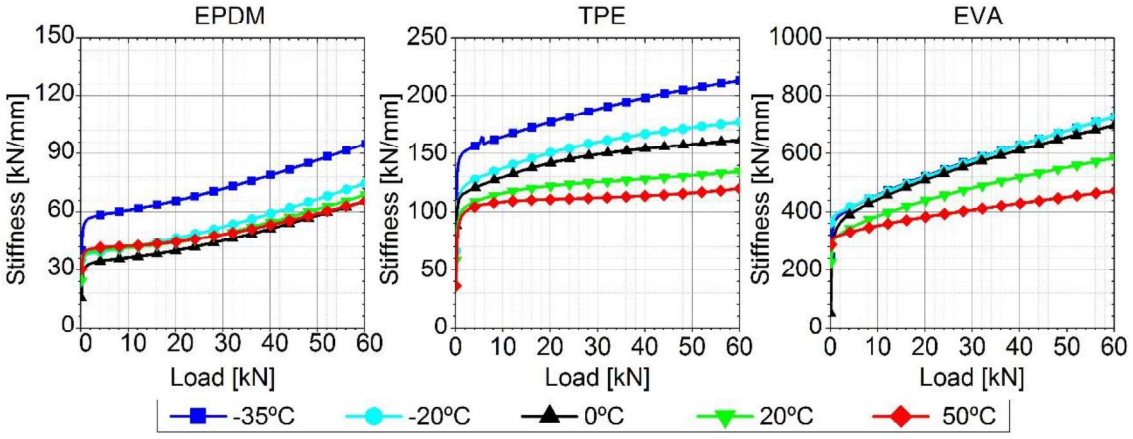


*Figure 9: Influence of temperature on relative static stiffness*

The influence of toe load ($F_{initial}$) and an increasing load range ($F_{final}=F_{final}+F_{range}$) on the relative static stiffness for the reference conditions (at a temperature of 20 °C) for the three rail pads, is shown in Figure 10. In general, an increase in toe load produces an increase in vertical stiffness. The specific response is, however, a material dependent property. This stiffness increase of the pads with toe load can be explained by analysing Figure 7. For the three materials it can be seen that in the first load section the greatest displacements occur and that, throughout the test, the slope of the curves increases. Therefore, it is evident that, when increasing the toe load, the deformation of the rail pads reduces for the same load. In Figure 10, it can also be observed that EPDM and TPE exhibit different curve profiles. This is because, in the former, the influence of the toe load is only of relevance for large load ranges while, in TPE, the stiffness differences attenuate as the load increases. In the case of EVA pads, the effect of the toe load is noticeable and uniform throughout the entire load range analysed.

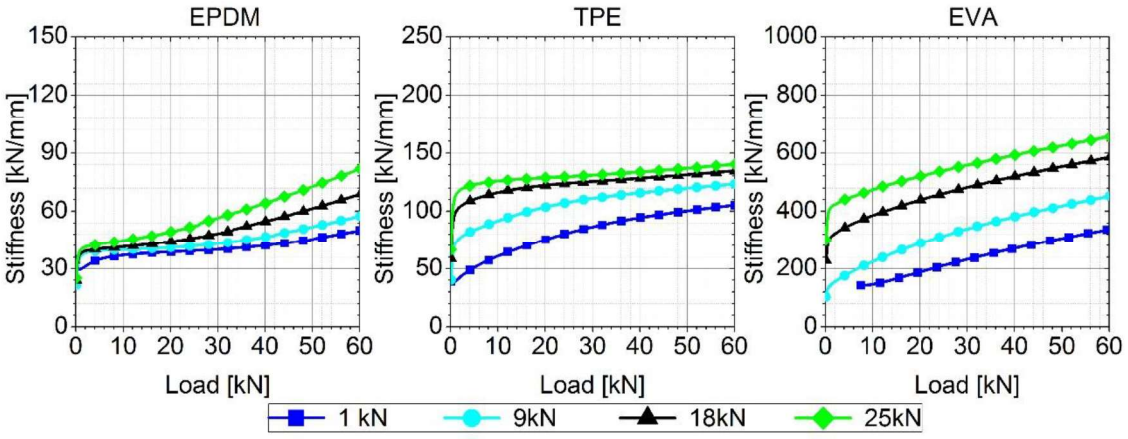


*Figure 10: Influence of the toe load on the relative static stiffness*

## 4.2. Dynamic Characterization

In the dynamic tests, the force-displacement curves of the three pad materials subjected to the reference conditions for high-speed rail are compared, see Figure 11. EPDM is the most flexible and energy dissipating rail pad per cycle, followed by TPE and finally EVA. This behaviour agrees with what was observed from the static tests in Figure 7.

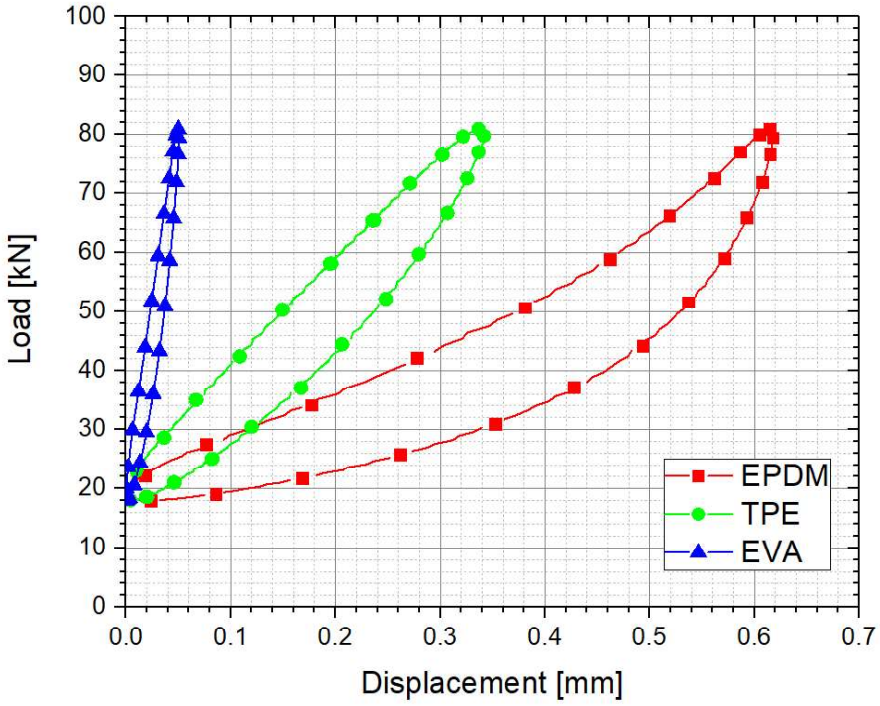


*Figure 11: Comparison of the dynamic stiffness of the three rail pads under reference conditions*

If we compare the static tests (Figure 7) with the dynamic tests (Figure 11), it can be seen that in all cases, for the same load value, the dynamic tests involve fewer displacements than the static tests. The rail pad in which this effect is greatest is the EVA one, which increases by 213%. While the other two rail pads behave in a similar way, 148% in the case of EPDM and 136% in the case of TPE.

The influence of temperature on the rail pads' dynamic stiffness is shown in Figure 12. This phenomenon is explained in the same way as the static stiffness. The response of the materials

to temperature variation displays dissimilar patterns. On the one hand, the force-displacement curves of EPDM are not influenced by temperature in the range between 0° C and 52 °C. However, its stiffness substantially increases at -20° C and even more at -35° C. In TPE, the dynamic stiffness increases gradually when temperature is reduced. In contrast, EVA pads are barely affected by temperature variations.

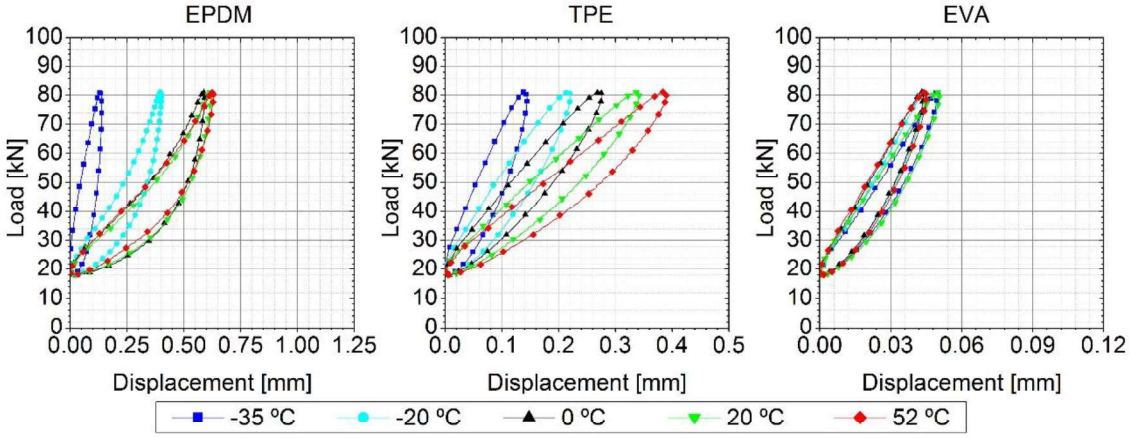


*Figure 12: Influence of temperature on dynamic stiffness of pads*

The influence of the axle load amplitude on the force-displacement curves of the rail pads is shown in Figure 13. It can be observed that as the axle load increases, the dynamic stiffness of the rail pads increases. This can be explained in a similar manner as the toe load influence, i.e., the higher the load that the rail pad supports, the smaller is the displacement per unit load. Note that the slope of the curves for TPE and EVA is hardly affected. Although the stiffness hardly changes, it can be seen that the hysteresis does increase significantly in all cases.

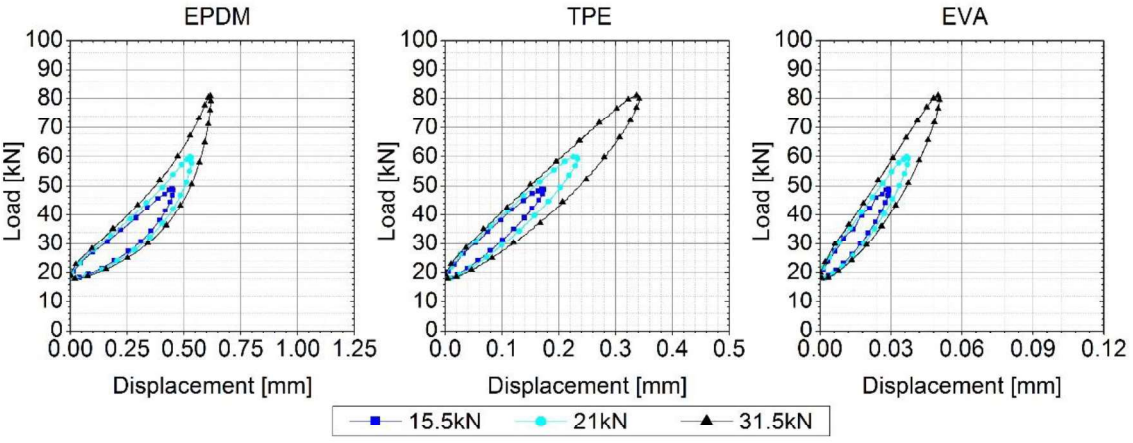


*Figure 13: Influence of the axle load amplitude on the pads' dynamic stiffness*

The influence of the toe load on the pads' dynamic stiffness is shown in Figure 14. It can be observed that the increment of toe load increases the stiffness of the rail pads, which is in line with the effect already observed in the static tests. The toe load affects the three rail pads in a significantly different manner. For EPDM, the maximum displacement substantially increases when the toe load is reduced. For this rail pad, it is also worth mentioning the noticeable increment in the dissipated energy when the toe load is 1 kN. The TPE is not greatly affected by the toe load, except when it is 1 kN. The same effect is present, in a more pronounced way for the EVA pad.

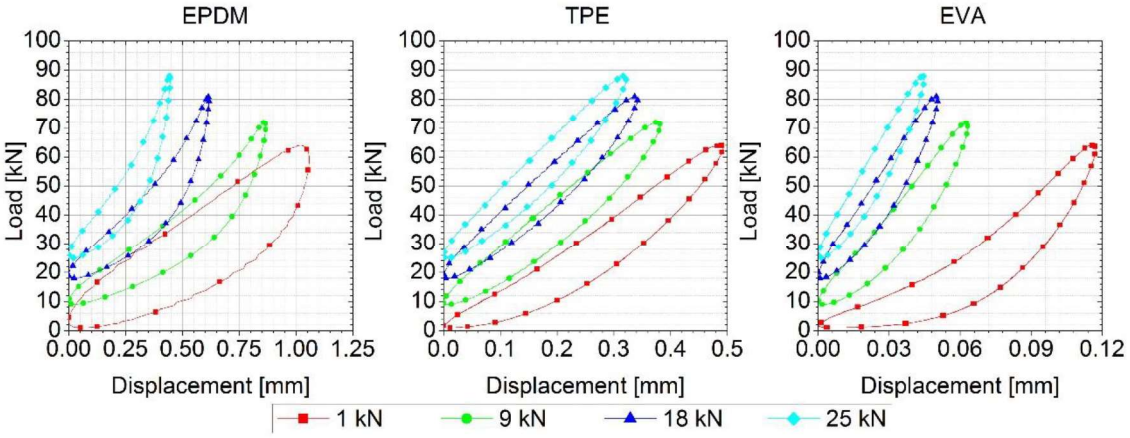


*Figure 14: Influence of the toe load on the pads' dynamic stiffness*

Figure 15 shows the influence of frequency on the pads' dynamic stiffness. It is observed that as frequency increases, the stiffness of rail pads increases and more energy is dissipated per cycle. The main reason for this is that as the speed of the test increases, the rail pad is no longer able to deform at the same speed. With respect to the increase in the dissipated energy when increasing the frequency of the test, this is because when accelerating the test, the polymer chains do not have time to reorganize, so when the test is carried out there is greater internal friction that dissipates more energy per cycle. The increase in frequency affects the three rail pads in a similar way, slightly increasing the stiffness of the rail pads but significantly enhancing the capacity to dissipate energy per cycle.

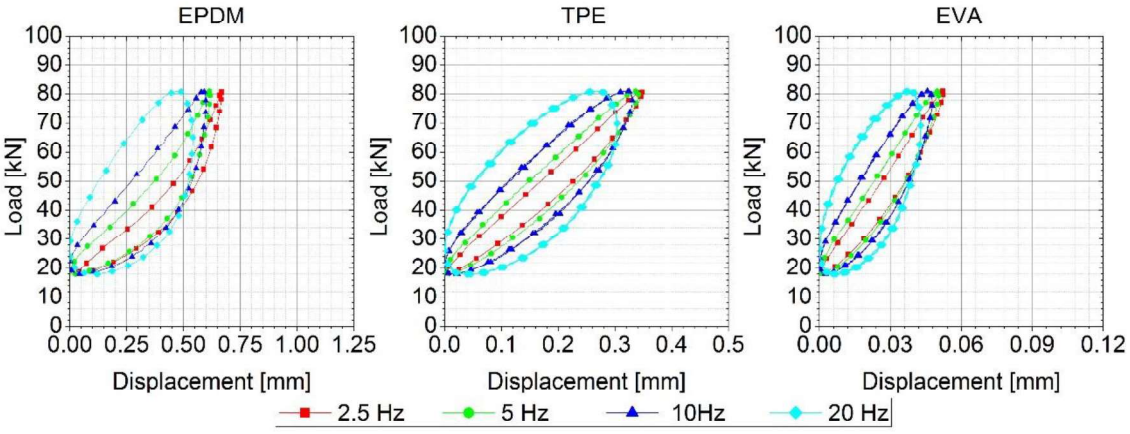


*Figure 15: Influence of the frequency on the pads' dynamic stiffness*

In this work an additional lab test is performed to understand the singular evolution of the dynamic stiffness of EPDM. The pad was subjected to a sinusoidal fatigue test with 40 kN mean load, 35 kN amplitude and frequency of 5 Hz. A thermocouple was fixed to the rail pad to record the evolution of its temperature. The test started at room temperature (26 °C) and the temperature of the environmental chamber was decreased at a rate of 1 °C/min. Force and displacements were recorded and, from these, the evolution of the stiffness was obtained, as shown in Figure 16. It can be observed that the dynamic stiffness remains approximately constant until 0 °C and increases gradually between 0 °C and -30 °C. Below this temperature the stiffness of the EPDM exhibits an abrupt and noticeable increase. These values agree with previous results obtained by Wei et al (Wei et al., 2017a), who observed that the static stiffness

of an EPDM pad increased when the temperature was below -10°C and that below -20°C this stiffening is accelerated.

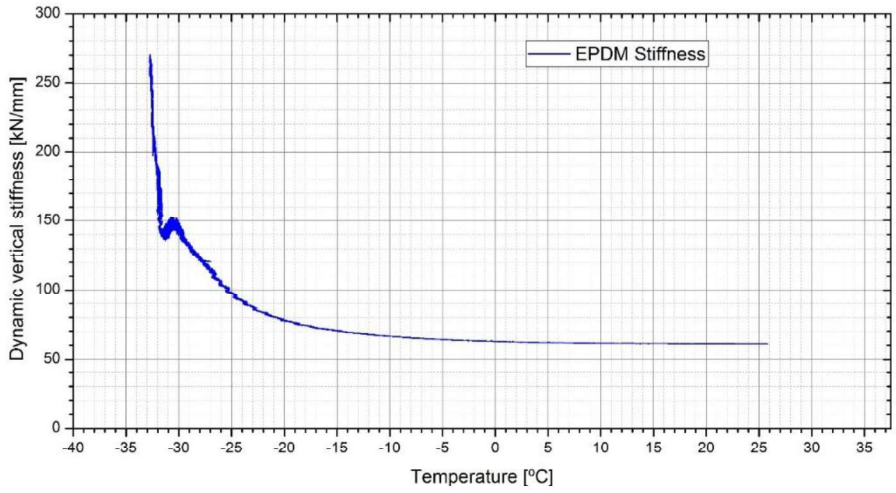


*Figure 16: Influence of temperature in the dynamic stiffness of EPDM*

Table 2 to Table 5 show the values of the influence coefficient CI, defined in equation (4), for each one of the four parameters analysed in this work with respect to the reference conditions for high-speed railway, i.e., temperature of 20 °C, axle load amplitude of 31.5 kN, toe load of 18 kN and frequency of 5 Hz.

*Table 2: Influence coefficient of the temperature on the dynamic vertical stiffness of the pads*

| Temperature [°C] | -35 | -20 | 0 | 52 |
|---|---|---|---|---|
| EPDM | 5.15 | 1.60 | 1.05 | 0.96 |
| TPE | 2.39 | 1.56 | 1.24 | 0.87 |
| EVA | 1.01 | 1.14 | 1.15 | 1.12 |

*Table 3: Influence coefficient of the axle load amplitude on the dynamic vertical stiffness of the pads*

| Axle Load Amplitude [kN] | 15.5 | 21.0 |
|---|---|---|
| EPDM | 0.65 | 0.76 |
| TPE | 0.98 | 0.98 |
| EVA | 0.84 | 0.90 |

*Table 4: Influence coefficient of the toe load on the dynamic vertical stiffness of the pads*

| Toe load [kN] | 1 | 9 | 25 |
|---|---|---|---|
| EPDM | 0.54 | 0.69 | 1.41 |
| TPE | 0.74 | 0.91 | 1.06 |
| EVA | 0.5 | 0.81 | 1.12 |

*Table 5: Influence coefficient of the frequency on the dynamic vertical stiffness of the pads*

| Frequency [Hz] | 2.5 | 10 | 20 |
|---|---|---|---|
| EPDM | 0.86 | 1.02 | 1.07 |
| TPE | 0.94 | 1.03 | 1.13 |
| EVA | 0.87 | 1.05 | 1.17 |

Table 6 shows the degree of influence of each parameter on the rail pads analysed here. The criterion used to assign these degrees of influence was the influence coefficient. A low degree implies variations of CI less than 10%, a medium degree corresponds to variations between 10 and 25% and a high degree is associated with variations of CI greater than 25%.

*Table 6: Degree of influence of each parameter on the dynamic stiffness of the pads*

| Parameter | EPDM | TPE | EVA |
|---|---|---|---|
| Temperature | High (if temperature is low) | High | Low-Medium |
| Amplitude | High | Low | Medium |
| Toe load | High | Low-Medium | High-Medium |
| Frequency | Low-Medium | Low-Medium | Low-Medium |

# 5. Conclusions

The characterization of the fastening system is of great relevance to study rail vehicle and track dynamics since the mechanical response depends almost exclusively on the vertical stiffness of the infrastructure, especially in slab tracks. In this context, the rail pads are the most problematic elements to characterize as they display high non-linearities and variability with the environmental and loading conditions. In this work, dedicated lab experiments on rail pads were performed in order to characterize their mechanical properties.

The experimental study comprised a total of 15 static and 720 dynamic tests carried out to measure and analyse the influence of the in-service conditions on the static and dynamic stiffness of three widely employed types of rail pads, namely, EPDM, TPE and EVA. Static vertical stiffness is the most commonly used parameter both for the design and for the classification of rail pads. In fact, regulations and technical specifications establish limit values on static stiffness. This approach is questionable since, under in-service conditions, it is the dynamic stiffness of the rail pads that best describes the response of the fastening system under the service loads. For this reason, the experimental study proposed here has focused on the influence that the actual operating conditions may exert on the dynamic stiffness. The operational variables studied were the temperature, axle load, toe load and frequency. The experimental results show that all these factors influence the stiffness of rail pads but the specific impact of each variable is strongly material-dependent. The main conclusions of the study are summarized hereafter:

- An increase in temperature causes reductions in the static and dynamic stiffness regardless of the material analysed. This pattern of behaviour is expected in polymeric materials. However, the specific details of the stiffness variations strongly depend on the rail pad. By fixing the rest of the variables at the reference standard values, the stiffness changes observed in EPDM, TPE and EVA when decreasing the temperature from 52°C to -35°C are, respectively, 437%, 173% and 11% of the stiffness at the maximum temperature (52°C). These results show the high sensitivity to thermal variation, especially of EPDM and TPE. The temperature was found to have a low influence on EPDM when the temperature is above -10°C, below which point the stiffness increases rapidly. TPE, on the other hand, shows a uniform variation in dynamic stiffness as the temperature varies. Finally, EVA shows thermostable behaviour.
- It has been observed that the increase of axle load (between 15.5 and 31.5 kN) is systematically accompanied by growth in the static and dynamic stiffnesses. Each of the rail pads, however, displays a specific level of sensitivity to this influence. The variations between the maximum and minimum values of dynamic stiffness, taking the latter as

the reference and setting the rest of the variables at their reference values, are 53%, 3% and 11% for EPDM, TPE and EVA, respectively. In this case, EPDM has the greatest sensitivity to variations of the axle load.

- The toe loads applied on the rail pads were varied between 1 and 25 kN. In this scenario, all rail pads have undergone increases in stiffness, both static and dynamic, after augmenting the toe load. The variations observed in the dynamic stiffness are strongly material-dependent. Thus, the changes measured between the maximum and minimum stiffness values, with respect to the minimum, are 159% for the EPDM, 42% for the TPE and 126% for the EVA.
- The influence of frequency, in the range between 2.5 Hz and 20 Hz, on the dynamic stiffness of the three rail pads showed similar results. Systematically, as frequency increases, the rail pads stiffen. The observed stiffness variations, referred to the minimum value, are similar, i.e., 24% for EPDM, 19% for TPE and 34% for EVA. It can also be seen that in all cases the dynamic stiffness is higher than the static stiffness.
- The variables that do not depend on the train, toe load and temperature, have a greater influence on both static and dynamic stiffness than those that do depend on it, axle load and frequency.

It is clear, therefore, that the variables evaluated in this study (temperature, frequency, axle and toe loads) have an important influence on the stiffness of rail pads. Therefore, the characterization procedure currently in use, established by the regulations, has limitations since it establishes standard characterization conditions, ignoring the high variability that is present under service conditions. The experimental results obtained from this work are very valuable as they have been obtained for three materials widely used by the rail industry and under a wide variety of operational conditions. This information is useful from several perspectives. First, for appropriate decision-making, based on experimental evidence. Secondly, it opens up perspectives for the development of novel models to predict the stiffness of rail pads from the operating conditions. In this regard, machine learning methods could play a prominent role. Finally, the data obtained in this work are likely to be implemented in numerical models to better predict the behaviour of the vehicle-track interaction. The implementation of degradation models to predict the long-term behaviour of the track can also support the development of decision support tools to enhance the performance optimization and maintenance procedures of rail tracks, contributing to reducing the life-cycle-costs of the infrastructure.

# Acknowledgements

This work was supported by FCT, through IDMEC, under LAETA, project UIDB/50022/2020.

# References

ADIF, 2005a. ET 03.360.570.0 Placas elásticas de asiento para sujeción VM.

ADIF, 2005b. PLACAS ELÁSTICAS DE ASIENTO PARA SUJECIÓN VM.

Carrascal, I.A., Pérez, A., Casado, J., Diego, S., Polanco, J.A., Ferreño, D., Martín, J.J., 2018. Experimental study of metal cushion pads for high speed railways. Constr. Build. Mater. 182, 273–283. https://doi.org/10.1016/j.conbuildmat.2018.06.134

Chen, J., Zhou, Y., 2020. Dynamic vertical displacement for ballastless track-subgrade system under high-speed train moving loads. Soil Dyn. Earthq. Eng. 129, 105911. https://doi.org/10.1016/J.SOILDYN.2019.105911

Coleman, I., Kassa, E., Smith, R., 2012. Wheel-Rail Contact Modelling within Switches and Crossings. Int. J. Railw. Technol. 1, 45–66. https://doi.org/10.4203/ijrt.1.2.3

Cukrowicz, K.C., Jahn, D.R., Graham, R.D., Poindexter, E.K., Williams, R.B., 2013. Suicide risk in older adults: Evaluating models of risk and predicting excess zeros in a primary care sample. J. Abnorm. Psychol. 122, 1021–1030. https://doi.org/10.1037/a0034953

Esveld, C., 2003. Developments in High-Speed Track Design. IABSE Symp. Rep. 87, 37–45. https://doi.org/10.2749/222137803796328782

Fenander, Å., 1997. Frequency dependent stiffness and damping of railpads. Proc. Inst. Mech. Eng. Part F J. Rail Rapid Transit 211, 51–62. https://doi.org/10.1243/0954409971530897

Ferreño, D., Casado, J., Carrascal, I.A., Diego, S., Ruiz, E., Saiz, M., Sainz-Aja, J., Cimentada, A.I., 2019. Experimental and finite element fatigue assessment of the spring clip of the SKL-1 railway fastening system. Eng. Struct. 188, 553–563. https://doi.org/10.1016/j.engstruct.2019.03.053

Fortunato, E., Paixão, A., Calçada, R., 2013. Railway Track Transition Zones: Design, Construction, Monitoring and Numerical Modelling. Int. J. Railw. Technol. 2, 33–58. https://doi.org/10.4203/ijrt.2.4.3

Indraratna, B., Nimbalkar, S., Rujikiatkamjorn, C., 2013. Modernisation of Rail Tracks for Higher Speeds and Greater Freight. Int. J. Railw. Technol. 2, 1–20. https://doi.org/10.4203/ijrt.2.3.1

Iwnicki, S.D., Bevan, A.J., 2012. Damage to Railway Wheels and Rails: A Review of the Causes, Prediction Methods, Reduction and Allocation of Costs. Int. J. Railw. Technol. 1, 121–146. https://doi.org/10.4203/ijrt.1.1.6

Kaewunruen, S., Remennikov, A.M., 2007. Response and Prediction of Dynamic Characteristics of Worn Rail Pads Under Static Preloads, in: Proceedings of 14th International Congress on Sound and Vibration. Australian Acoustics Society, Cairns, Australia, pp. 1–8.

Kaewunruen, S., Remennikov, A.M., 2006. Sensitivity analysis of free vibration characteristics of an in situ railway concrete sleeper to variations of rail pad parameters. J. Sound Vib. 298, 453–461. https://doi.org/10.1016/j.jsv.2006.05.034

Li, X., Nielsen, J.C.O., Torstensson, P.T., 2019. Simulation of wheel-rail impact load and sleeper-ballast contact pressure in railway crossings using a Green's function approach. J. Sound Vib. 463, 114949. https://doi.org/10.1016/j.jsv.2019.114949

Li, X., Torstensson, P.T., Nielsen, J.C.O., 2017. Simulation of vertical dynamic vehicle–track interaction in a railway crossing using Green's functions. J. Sound Vib. 410, 318–329. https://doi.org/10.1016/j.jsv.2017.08.037

Markine, V.L., Steenbergen, M.J.M.M., Shevtsov, I.Y., 2011. Combatting RCF on switch points by tuning elastic track properties. Wear 271, 158–167. https://doi.org/10.1016/J.WEAR.2010.10.031

Marques, F., Magalhães, H., Liu, B., Pombo, J., Flores, P., Ambrósio, J., Piotrowski, J., Bruni, S., 2019. On the generation of enhanced lookup tables for wheel-rail contact models. Wear 434–435, 202993. https://doi.org/10.1016/j.wear.2019.202993

Peltokangas, O., Nurmikolu, A., 2015. Evolution of Railway Track Settlement after Ballast Tamping. Int. J. Railw. Technol. 4, 1–18. https://doi.org/10.4203/ijrt.4.2.1

Pombo, J., Ambrósio, J., 2012. An alternative method to include track irregularities in railway

vehicle dynamic analyses. Nonlinear Dyn. 68, 161–176. https://doi.org/10.1007/s11071-011-0212-2

Pombo, J., Ambrósio, J., 2008. Application of a wheel–rail contact model to railway dynamics in small radius curved tracks. Multibody Syst. Dyn. 19, 91–114. https://doi.org/10.1007/s11044-007-9094-y

Pombo, J., Ambrósio, J., Silva, M., 2007. A new wheel–rail contact model for railway dynamics. Veh. Syst. Dyn. 45, 165–189. https://doi.org/10.1080/00423110600996017

Sadeghi, J., Seyedkazemi, M., Khajehdezfuly, A., 2020. Nonlinear simulation of vertical behavior of railway fastening system. Eng. Struct. 209, 110340. https://doi.org/10.1016/J.ENGSTRUCT.2020.110340

Sadri, M., Lu, T., Steenbergen, M., 2019. Railway track degradation: The contribution of a spatially variant support stiffness - Local variation. J. Sound Vib. 455, 203–220. https://doi.org/10.1016/J.JSV.2019.05.006

Sainz-Aja, J., Carrascal, I., Polanco, J.A., Thomas, C., Sosa, I., Casado, J., Diego, S., 2019. Self-compacting recycled aggregate concrete using out-of-service railway superstructure wastes. J. Clean. Prod. 230, 945–955. https://doi.org/10.1016/j.jclepro.2019.04.386

Sainz-Aja, J., Pombo, J., Tholken, D., Carrascal, I., Polanco, J., Ferreño, D., Casado, J., Diego, S., Perez, A., Filho, J.E.A., Esen, A., Cebasek, T.M., Laghrouche, O., Woodward, P., 2020. Dynamic calibration of slab track models for railway applications using full-scale testing. Comput. Struct. 228, 106180. https://doi.org/10.1016/j.compstruc.2019.106180

Sañudo, R., Markine, V., Pombo, J., 2017. Study on Different Solutions to Reduce the Dynamic Impacts in Transition Zones for High-Speed Rail. J. Theor. Appl. Vib. Acoust. 3, 199–222. https://doi.org/10.22064/tava.2018.80091.1095

Sol-Sánchez, M., Moreno-Navarro, F., Rubio-Gámez, M.C., 2015. The use of elastic elements in railway tracks: A state of the art review. Constr. Build. Mater. 75, 293–305. https://doi.org/10.1016/j.conbuildmat.2014.11.027

Stichel, S., Jönsson, P.-A., Casanueva, C., Hossein Nia, S., 2014. Modelling and Simulation of Freight Wagon with Special attention to the Prediction of Track Damage. Int. J. Railw. Technol. 3, 1–36. https://doi.org/10.4203/ijrt.3.1.1

Vollebregt, E.A.H., Steenbergen, M.J.M.M., 2015. A Methodology for Assessing Track Irregularities with respect to Rail Damage. Int. J. Railw. Technol. 4, 85–105. https://doi.org/10.4203/ijrt.4.4.5

Wei, K., Liu, Z., Liang, Y., Wang, P., 2017a. An investigation into the effect of temperature-dependent stiffness of rail pads on vehicle-track coupled vibrations. Proc. Inst. Mech. Eng. Part F J. Rail Rapid Transit 231, 444–454. https://doi.org/10.1177/0954409716631786

Wei, K., Wang, F., Wang, P., Liu, Z., Zhang, P., 2017b. Effect of temperature- and frequency-dependent dynamic properties of rail pads on high-speed vehicle–track coupled vibrations. Veh. Syst. Dyn. 55, 351–370. https://doi.org/10.1080/00423114.2016.1267371

Wei, K., Zhang, P., Wang, P., Xiao, J., Luo, Z., 2016. The Influence of Amplitude- and Frequency-Dependent Stiffness of Rail Pads on the Random Vibration of a Vehicle-Track Coupled System. Shock Vib. 2016, 1–10. https://doi.org/10.1155/2016/7674124

Xin, T., Ding, Y., Wang, P., Gao, L., 2020. Application of rubber mats in transition zone between two different slab tracks in high-speed railway. Constr. Build. Mater. 243, 118219.

https://doi.org/10.1016/J.CONBUILDMAT.2020.118219

Zhu, S., Cai, C., Luo, Z., Liao, Z., 2015. A frequency and amplitude dependent model of rail pads for the dynamic analysis of train-track interaction. Sci. China Technol. Sci. 58, 191–201. https://doi.org/10.1007/s11431-014-5686-y